Evaluation of S2 alar and traditional S1 pedicle fixation for severe lumbar spondylolisthesis in different bone mineral densities: a finite element analysis

Juehan Wang[1†],Wei Chen[1,2†],Xi Yang[1],Ce Zhu[1],Tingxian Ling[1],Ganjun Feng[1],Yueming Song[1],Limin Liu[1*]

* Corresponding author, Correspondence: liulimin_spine@163.com

†Juehan Wang and Wei Chen contributed equally to this work.

[1]Department of Orthopedic Surgery and Orthopedic Research Institute, West China Hospital, Sichuan University, No. 37 GuoXue Road, Chengdu, Sichuan, China.

[2] Department of Orthopedic Surgery, Panzhihua Central Hospital, Panzhihua 617000, PR China.

Abstract

Background: Lumbar spondylolisthesis is a common disease in older populations. The surgical treatment of spondylolisthesis has a history of more than 50 years, with L5-S1 screws widely used in clinical practice to reduce slippage and fusion. However, some patients with severe lumbar spondylolisthesis and

osteoporosis could have complications, such as internal fixation rupture, S1 screw loosening, and incomplete slippage reduction. To better treat this kind of patient, sacral screw fixation is gradually becoming more common. Little is known about the biomechanical performance of L5-S2 alar internal fixation constructs after posterior lumbar interbody fusion. This study aimed to compare L5-S1 reduction and fixation methods and explore whether extending the fixation to include the S2 alar can significantly improve the stability of the internal fixation device.

METHODS: Two kinds of validated finite element models of the L5-S1 segment were reconstructed via computed tomography images, including (1) the L5-S1 screw fixation model and (2) the L5-S2 alar fixation model. The inverse repair was performed using Geomagic software, the internal fixation device was drawn using Creo software, and the model parameters were set and analyzed using ANSYS Workbench software.

Results: The average load of the L5-S2 alar internal fixation device was 86.9-111% higher than that of the L5-S1 fixation device when the internal bone of the S1 screw canal yielded. In the L5-S1 fixation model, the stress was concentrated in the tail of the S1 screw, and in the L5-S2 alar fixation model, the stress was concentrated in the titanium rod. In the L5-S2 alar fixation method, the internal deformation of the S1 screw track was scattered and uniform, while in the L5-S1 fixation method, local bone destruction in the front and back ends of the screw track was prone to occur due to the stress concentration.

Conclusion: Extending fixation to the S2 wing can significantly improve internal fixation device stability and reduce the risk of intraoperative and postoperative fractures while avoiding injury to the sacroiliac joint, reducing the difficulty of surgery and the risk of injury to surrounding tissues. It is a reasonable plan for the treatment of moderate and severe lumbar spondylolisthesis with osteoporosis.

Key words: Spondylolisthesis, Osteoporosis, S2 alar screw, Finite element analysis

Introduction

Lumbar spondylolisthesis is a deformity that occurs between the lumbar vertebrae and the relative adjacent vertebrae, mainly consists of horizontal displacement, and is one of the most common spinal deformities. Wiltse et al. classified lumbar spondylolisthesis into six types based on the causative factors: dysplastic, isthmic, degenerative, traumatic, pathological and iatrogenic [1]. Severe lumbar spondylolisthesis may result in lumbar curvature changes, nerve compression, and decreased lumbar spine stability. Patients can present obvious symptoms of low back pain and often require surgical treatment. The main objectives of surgical treatment are to restore lumbar spine stability, relieve nerve strain and compression, and improve clinical symptoms.

In 1986, Matthiass proposed lever reduction using pedicle screws and a rod fixation system [2]. Since then, with the development of internal fixation materials and

clinical practice, the application of pedicle screws in the treatment of lumbar spondylolisthesis has gradually become widespread. However, problems such as screw loosening, iatrogenic fracture and broken internal fixation devices have not been satisfactorily solved, especially screw loosening in osteoporotic patients. Severe osteoporosis is a significant cause of internal fixation failure, such as pedicle screw loosening and pull-out after spinal fusion surgery [3-5]. Spondylolisthesis often occurs in the L5/S1 segment because there is a high degree of mobility at the L4-S1 segment, joining the rigid sacropelvic unit. Failure of instrumentation frequently begins at the sacrum, which is the site of maximum stress [6]. The reported failure rate of S1 pedicle screws is approximately 44% [6-8]. Thus, extension of the instrumentation to the distal sacrum or iliac wings has gained increasing interest. Alternatives to the single use of S1 screws include the addition of S2 alar screws and S2 alar-iliac screws.

Finite element analysis (FEA) is a mathematical and physical computational method that can analyze objects of various shapes by building multiple tiny units and simulating changes that occur during the stressing process [9]. FEA has already been applied to characterize the complex biomechanical properties of the lumbar vertebrae in previous studies [10,11]. Nevertheless, to the best of our knowledge, few studies have illustrated the detailed biomechanical mechanisms of L5-S1 and L5-S2 alar fixation in spondylolisthesis patients with osteoporosis.

The aim of this study is to compare L5-S1 reduction and fixation methods and explore whether extending the fixation to include the S2 alar can significantly improve the stability of the internal fixation device by FEA.

Materials and methods

Construction of the intact model

A 35-year-old healthy male volunteer with no history of lumbar disease was selected. Computed tomography (CT) images (Siemens Sensation 64, Siemens Medical Solutions, Forchheim, Germany) were acquired at 120 kVp and 200 mAs and provided by the Department of Radiology at The West China Hospital. The CT images were stored in Digital Imaging and Communications in Medicine (DICOM) format. Informed written consent was obtained from the subject participating in the study.

The collected raw data were imported into Mimics Research 19.0 (Materialise NV, Leuven, Belgium) for three-dimensional (3D) reconstruction. Subsequently, the 3D model generated by Mimics was imported into Geomagic Studio 2013 (3D Systems, Inc., Rock Hill, South Carolina, USA) to simulate the transforaminal lumbar interbody fusion (TLIF) surgical procedure by the application of facetectomy, annulotomy, and soft tissue release for lumbar spondylolisthesis. Using the toggle Mask 3D Preview option, the editMask command was applied to remove the lower articular process on both sides of the L5 vertebra and the upper articular process on

both sides of the S1 vertebra (Fig. 1). The spikes and features were deleted, smoothing was performed with a polygon mesh, and the triangles were made more uniform in size. Then, a patch was generated using the following tools: Construct Patches and Grid and Fit Surfaces. The smoothed model was saved and imported into ANSYS Workbench 19.0 (ANSYS, Ltd., Canonsburg, Pennsylvania, USA). Each vertebra was modeled as consisting of a cancellous inner core surrounded by a 1 to 1.5 mm cortical shell. A 0.5 mm bony end plate was simulated on either end of each vertebra (Fig. 2). The material properties of the various spinal components were derived from the literature [12-15], as specified in Table 1.

Component/Materials	Density (kg/m^3)	Young Modulus (MPa)	Poisson Ratio	yield stress (MPa)
Cancellous bone	160/240/320	57/143/267	0.2	2.2/3.9/5.9
Cortical bone	1910	12000	0.3	100
Spinal instrumentation (titanium alloy)	4430	110000	0.3	860

Table 1. Material Properties Used in the Finite Element Model

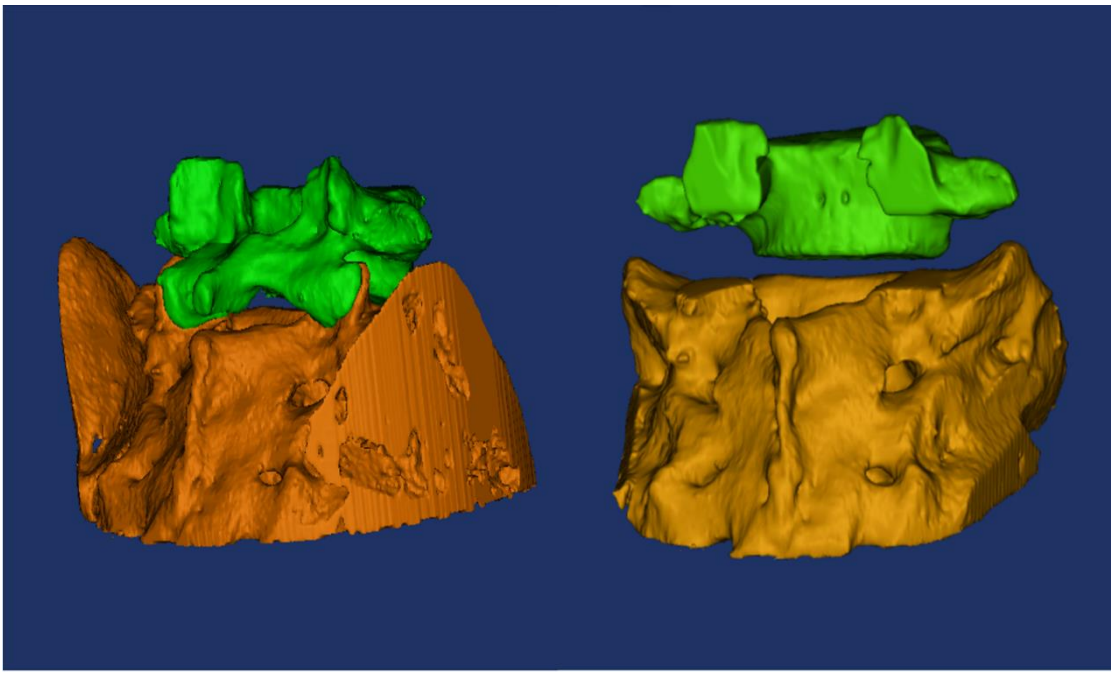

110 *Fig. 1: The original 3D lumbosacral model (left) and the final 3D lumbosacral model*

111 *after smoothing and editing.*

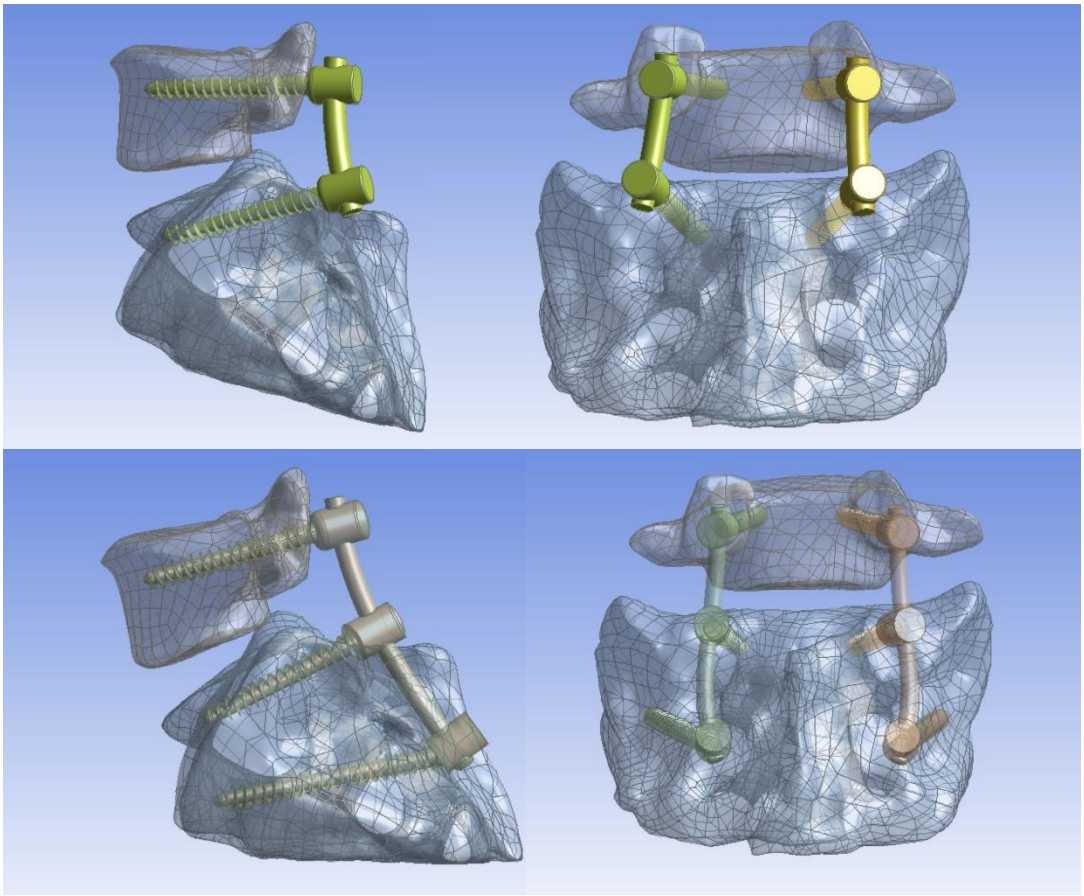

Fig. 2: Lateral (left panel) and posterior (right panel) views of the lumbosacral configurations investigated.

Modeling of implants

The posterior instrumentation consisted of transpedicular screws and longitudinal rods spanning between adjacent screws and was modeled by Creo Parametric 6.0 computer-aided design (CAD) (PTC, Boston, MA, USA). The L5 and S1 pedicle screws were 45 mm in length and 6 mm in diameter, and the S2 alar pedicle screws were 60 mm in length and 6 mm in diameter. Titanium material properties were applied for the posterior instrumentation.

Construction of models with two different fixation options and different bone mineral densities

The screws and rods were assembled with the lumbar spine model to construct the two models separately in ANSYS Workbench 19.0 (ANSYS, Ltd., Canonsburg, Pennsylvania, USA). Repeating the above simulated screw placement and subsequent steps, by fine-tuning the pedicle screw angle and depth, a total of 72 models were built, including 36 cases of L5-S1 fixation and 36 cases of L5-S2 alar fixation, and the bone mineral density (BMD) in each fixation model was divided into low, medium and high. The specific BMD values are shown in Table 1.

Contact definitions

A finite sliding algorithm with a coefficient of friction of 0.2 was defined between the pedicle screws and screw paths to allow for any small relative displacements. The pedicle screws were placed such that they engaged approximately two-thirds of the vertebral body.

Loading and boundary conditions

A motion protocol was defined for all reconstructive options and the intact lumbar spine condition. Both sides of the sacroiliac joint surface were immobilized throughout the load simulation. A sustained 150 N preload parallel to the L5 upper endplate was imposed on the bilateral L5 pedicle screws to simulate the intraoperative pull-out strength when the spondylolisthesis was reduced (Fig. 3). Screws were judged to have started to loosen when the average stress of the screw path bone was close to the yield stress. The yield load of the S1 screw path, the stress distribution of the two different internal fixation methods and the S1 bone deformation were analyzed and compared to investigate the biomechanical properties of L5-S1 fixation and L5-S2 alar fixation.

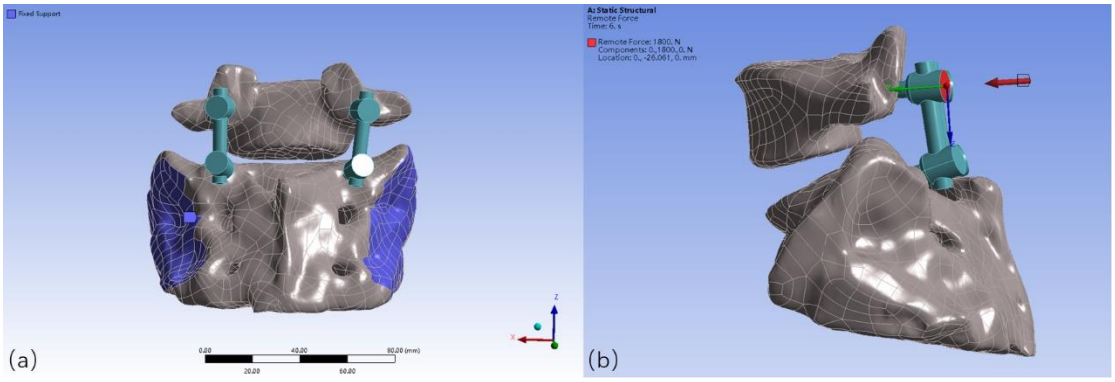

Fig. 3: Loading and boundary conditions set for the lumbosacral configurations investigated: (a) boundary conditions of the intact model (the purple area represents

the immobilized sacroiliac joint surfaces); (b) loading conditions (the red arrow represents the preload employed parallel to the L5 upper endplate).

Statistical analysis

Data were analyzed using SPSS 19.0 and are represented as the mean ± SD. Analysis of variance (ANOVA) or Student's t test was performed to measure the statistical significance of differences, and $P < 0.05$ was considered statistically significant.

Results

1. Yield load of the S1 screw path

In the L5-S1 fixation model, the S1 screw path stresses were unevenly distributed, with the main stresses concentrated on the upper contact surface at the tail of the screw path and the lower contact surface at the front of the screw path. Nevertheless, in the L5-S2 alar model, the stresses were relatively dispersed, and the main stresses were distributed at the caudal lateral side of the screw path (Fig. 4). In the low BMD model, when the bone of the S1 screw path reached the yield stress (2.2 MPa), the load in the L5-S1 model was 355.58±11.5 N, which was in accordance with previously reported data [16]. Meanwhile, the corresponding load of the L5-S2 alar model was approximately 664.75±9.2 N. In the medium BMD model, when the bone of the S1 screw path reached the yield stress (3.9 MPa), the corresponding load in the L5-S1 model was approximately 593.17±19.6 N, while the corresponding load

in the L5-S2 alar model was approximately 664.75±9.2 N. In the high BMD model, when the bone of the S1 screw path reached the yield stress (5.9 MPa), the corresponding load in the L5-S1 model was approximately 803.42±24.2 N. The corresponding load in the L5-S2 alar model was approximately 1695±23.4 N. A comparative analysis of the relevant data is shown in Table 2, and the corresponding relationship between the load and BMD is shown in Fig. 5.

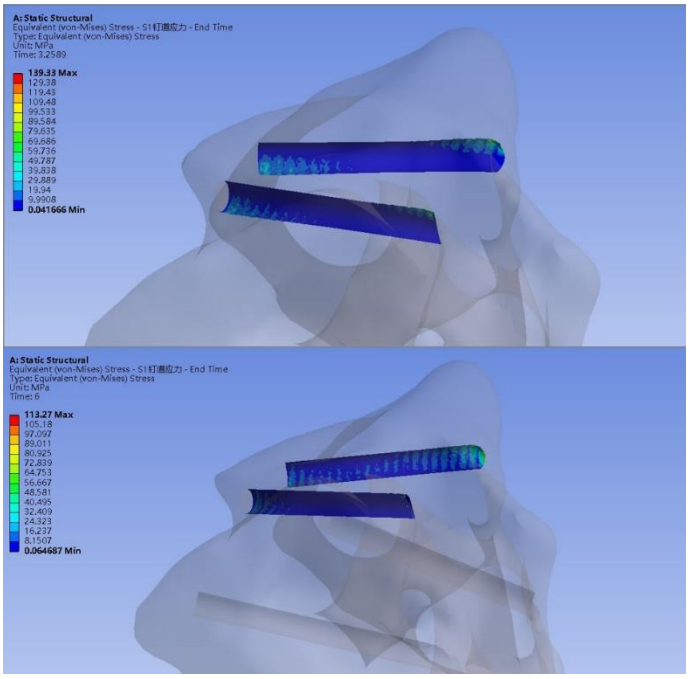

Fig. 4: Stress distribution of the S1 screw path. The figure above shows the L5-S1 model and the figure below shows the L5-S2alar model

Group	Cases	Low-BMD	Medium-BMD	High-BMD	F	*p*
L5-S1	36	355.58±11.5	593.17±19.6	803.42±24.2	1637.324	<0.001
L5-S2alar	36	664.75±9.2	1148.25±16.0	1695±23.4	10757.334	<0.001
t		72.579	75.965	91.698		
p		<0.001	<0.001	<0.001		
increasing rate		86.9%	93.6%	111%		

176 *Table 2: Comparison of the yield load of the S1 screw path in the two groups of*

177 *models（$\bar{x}\pm s$，N）*

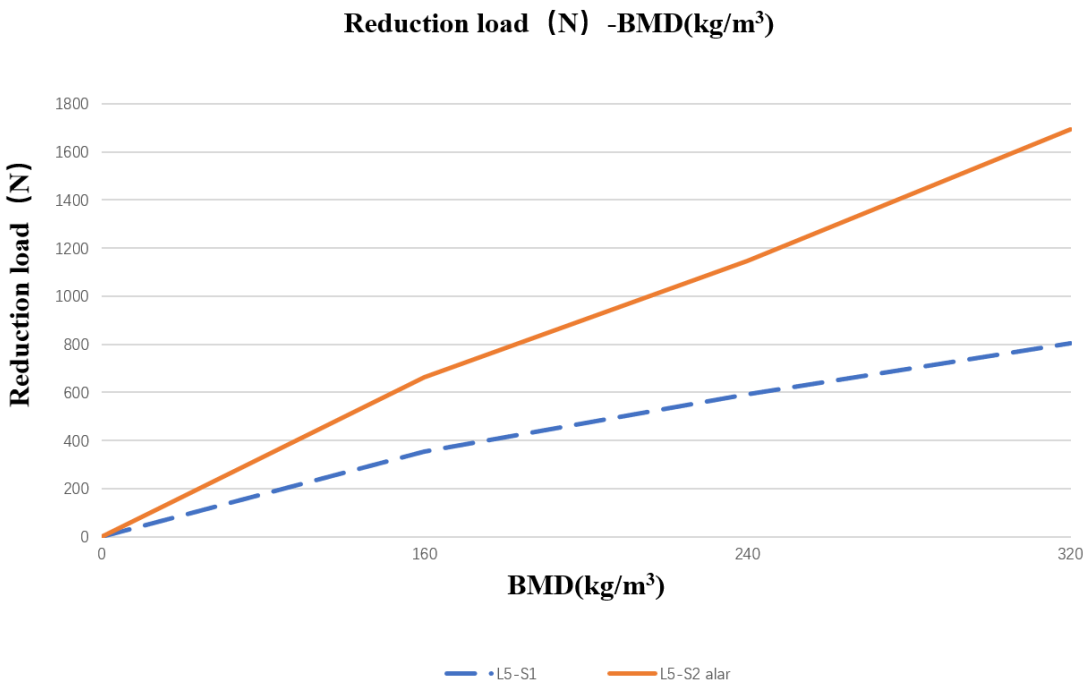

178

179 *Fig. 5: Correspondence between the reduction load and BMD. In the range below the*

180 *load-BMD curve of the L5-S1 model, the corresponding reduction load was relatively*

181 *low, and even L5-S1 fixation can achieve reliable fixation. Within the range between*

182 *the "L5-S1" curve and the "L5-S2 alar" curve, the required reduction load was*

moderate, and L5-S1 fixation could not provide good stability; therefore, the L5-S2 alar fixation method should be selected. In the range above the "L5-S2 alar" curve, the required load was too high, and even L5-S2 alar fixation could not provide reliable stability.

2. Stress of internal fixation

The internal fixation stress distribution of the L5-S1 model and the L5-S2 alar model is shown in Figure 3. In the L5-S1 model, the maximum stress was concentrated at the tail of the screw, while in the L5-S2 alar model, the maximum stress was concentrated on the connecting rod near the S1 screw (Fig. 6). In the low BMD model, when the S1 bone yielded, the stress at the tail of the L5-S1 model screws was approximately 421 MPa; meanwhile, the maximum stress of the L5-S2 alar model screws was approximately 226 MPa, and the maximum stress of the titanium rod was approximately 345 MPa. In the medium BMD model, when the S1 bone yielded, the L5-S1 model maximum stress was approximately 686 MPa; the L5-S2 alar model maximum stress was approximately 374 MPa, and the maximum stress of the titanium rod was approximately 594 MPa. In the high BMD model, when the S1 bone yielded, the maximum stress of the L5-S1 model was approximately 940 MPa, the maximum stress of the L5-S2 alar model was approximately 539 MPa, and

the maximum stress of the titanium rod was approximately 876 MPa. A statistical comparative analysis is shown in Table 3.

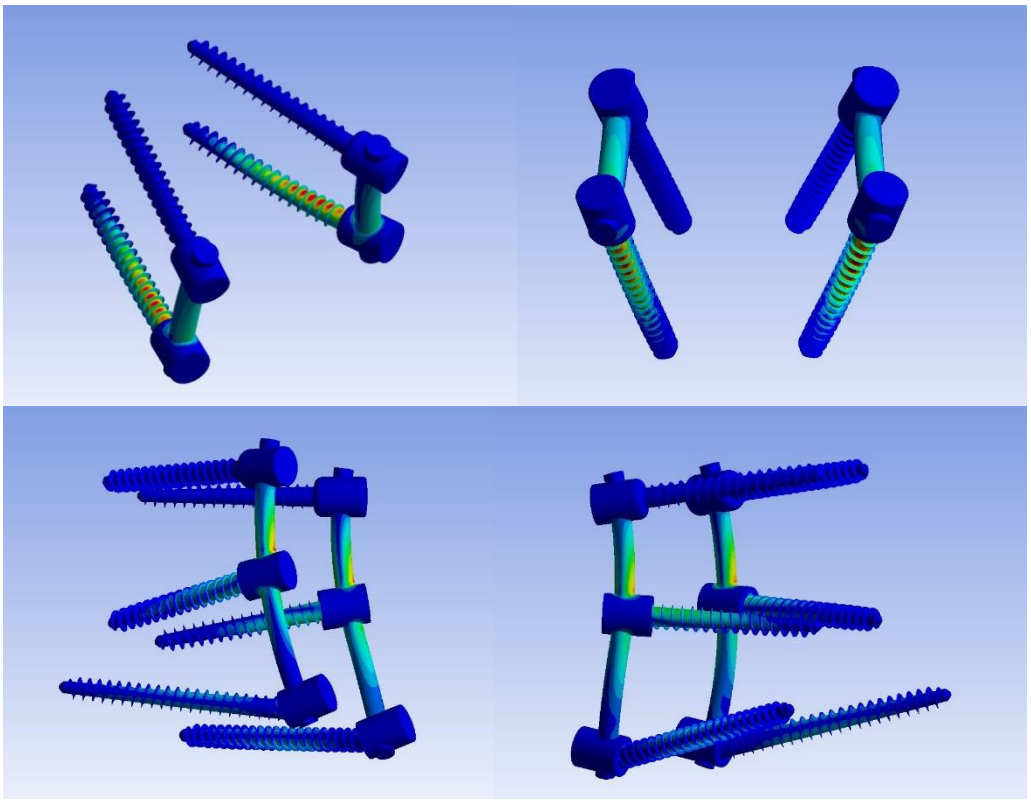

Fig. 6: Stress distribution of internal fixation in the two models. The figure above shows the L5-S1 model and the figure below shows the L5-S2alar model.

Group	Cases	Low-BMD	Medium-BMD	High-BMD	F	*p*
L5-S1	36	423.25±9.0	689.83±14.569	945.33±20.155	3496.572	＜0.001
L5-S2 alar	36	225.42±9.1	373.00±15.0	537.58±21.865	1115.909	＜0.001
t		53.646	52.271	47.498		
p		＜0.001	＜0.001	＜0.001		

Table 3: Comparison of the maximum stress of the S1 screw in the two groups of models（$\bar{x}\pm s$，MPa）

3. S1 screw path deformation

In the L5-S1 model, the most obvious deformation of the S1 path was on the upper contact surface of the tail, followed by the lower contact surface of the anterior segment of the screw path. The deformation of the middle and rear screw path was the least, and the internal and external deformation was similar. In the L5-S2 alar model, the largest deformation was located at the tail of the screw path, and the overall distribution was relatively uniform (Fig. 7). Regardless of BMD, when the S1 screw path bone yielded, the maximum deformation value of the screw path was similar in

both models (P>0.05), while the average deformation value of the screw path was significant different (P＜0.01), as shown in Tables 4 and 5.

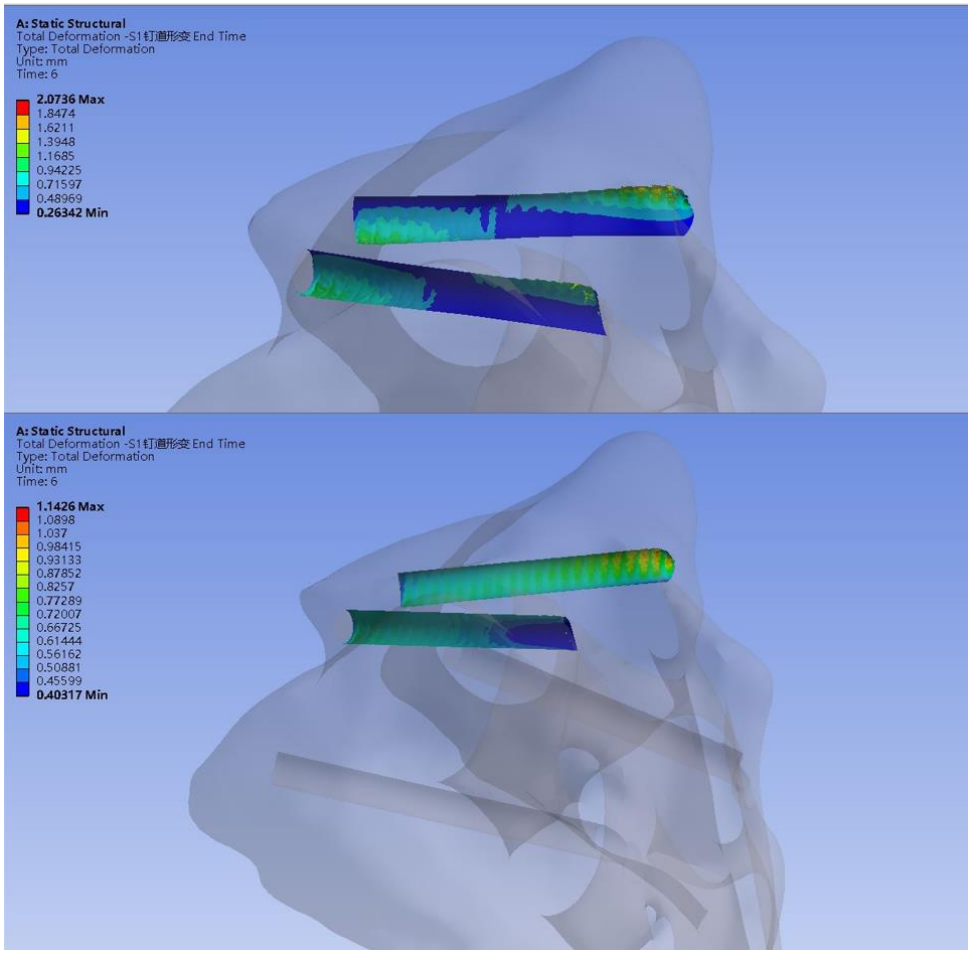

Fig. 7: Deformation distribution of the S1 screw path in the two groups of models under low BMD conditions. The figure above shows the L5-S1 model and the figure below shows the L5-S2alar model.

Group	Cases	Low-BMD	Medium-BMD	High-BMD
L5-S1	36	0.15±0.02	0.13±0.15	0.12±0.13
L5-S2 alar	36	0.24±0.01	0.24±0.01	0.24±0.01
t		17.594	21.432	26.238
p		＜0.001	＜0.001	＜0.001

220 *Table 4: Comparison of mean values of bone deformation in the two groups（$\bar{x}\pm s$，*

221 *mm）*

Group	Cases	Low-BMD	Medium-BMD	High-BMD
L5-S1	36	0.48±0.05	0.43±0.05	0.42±0.04
L5-S2 alar	36	0.46±0.02	0.43±0.02	0.41±0.02
t		1.171	0.292	0.372
p		＞0.05	＞0.05	＞0.05

222 *Table 5: Comparison of maximum values of bone deformation in the two groups*

223 *（$\bar{x}\pm s$，mm）*

224 # Discussion

225 Lumbar spondylolisthesis is a common disease treated by spinal surgery. Most

226 patients suffer from low back pain due to spinal stenosis, loss of spinal stability and

227 compression of nerve roots, which often require surgical treatment. Determined by the

physiological curvature and range of motion of the spine, the majority of spondylolisthesis is anterolisthesis. According to the Meyerding classification, when the vertebral displacement exceeds 50% of the adjacent lower vertebral body, moderate to severe slippage can be diagnosed.

In the current surgical treatment of lumbar spondylolisthesis, L5-S1 internal fixation is mostly reported for reduction; this method has been widely used for many years with proven efficacy, but it also has shortcomings. Due to the short force arm and relatively concentrated stress, this L5-S1 reduction method based on the lever principle is prone to S1 screw loosening in patients with moderate to severe spondylolisthesis, especially in the case of osteoporosis [17]. In response to this problem, surgical approaches continue to be explored and modified, including extended internal fixation to S2, sacroiliac joint fixation and iliac fixation [18]. From a biomechanical point of view, extended methods must be able to increase the stability of the internal fixation device and provide greater power for lifting and reduction. However, each extended internal fixation method still has some flaws. The use of sacroiliac screw fixation inevitably leads to sacroiliac joint damage, loss of sacroiliac joint mobility, and increased long-term risk of chronic sacroiliac pain [19]. Due to the anatomy of the S2 pedicle, which is relatively short and close to the anterior internal iliac artery, extended fixation to the S2 pedicle may lead to insufficient holding power, limited auxiliary ability and even possibly massive hemorrhage. The iliac screw fixation device has a complex structure and improves the risk of local soft tissue injury, chronic pain, and even skin breakdown. These complications are more

frequently reported in older patients with osteoporosis [20-22]. To the best of our knowledge, there is a paucity of studies that have examined the biomechanical differences between L5-S1 and L5-S2 alar fixation in severe spondylolisthesis with different BMDs.

This study presents a preliminary biomechanical evaluation of L5-S1 and L5-S2 alar fixation with different BMDs to analyze the intraoperative reduction stress distribution in severe lumbar spondylolisthesis patients with osteoporosis via FEA. Regarding the yield load of the S1 screw path, in the L5-S1 fixation method, when lifting and repositioning the site of lumbar spine slippage, the stress was concentrated on the tail of the S1 screw path. Because of the thinner cortex of the sacrum compared to that of other vertebrae, excessive concentrated stress could lead to screw loosening or even internal fixation failure. This may also explain why screw loosening often occurs in the tail segment. Nevertheless, in the S2 alar fixation method, the S1 screw path stress was uniformly distributed. When the bone in the S1 screw path yielded, the average load of the L5-S2 alar model was 86.9%-111% higher than that of the L5-S1 model, which could significantly improve the reduction ability and S1 screw stability, especially in the low BMD group. This result could be observed more visually in the reduction load-BMD diagram (Fig. 5). When the BMD and the load required for reduction were below the "L5-S1" line, fixation with both 4 screws and 6 screws could achieve reliable stability. However, when the BMD and the load required for reduction were between the "L5-S1" and the "L5-S2 alar" lines, the L5-S1 fixation method could lead to internal fixation failure or could not provide good sagittal

alignment, while the L5-S2 alar method could provide reliable reduction. This result can be of value in informing clinical practice. For instance, in a spondylolisthesis patient with severe osteoporosis treated in our department, ideal reduction was not achieved after L5-S1 fixation because of the inadequate lifting force, and compared to another patient with the same conditions, extended fixation to the S2 alar could obviously help him/her achieve better postoperative sagittal alignment (Fig. 8).

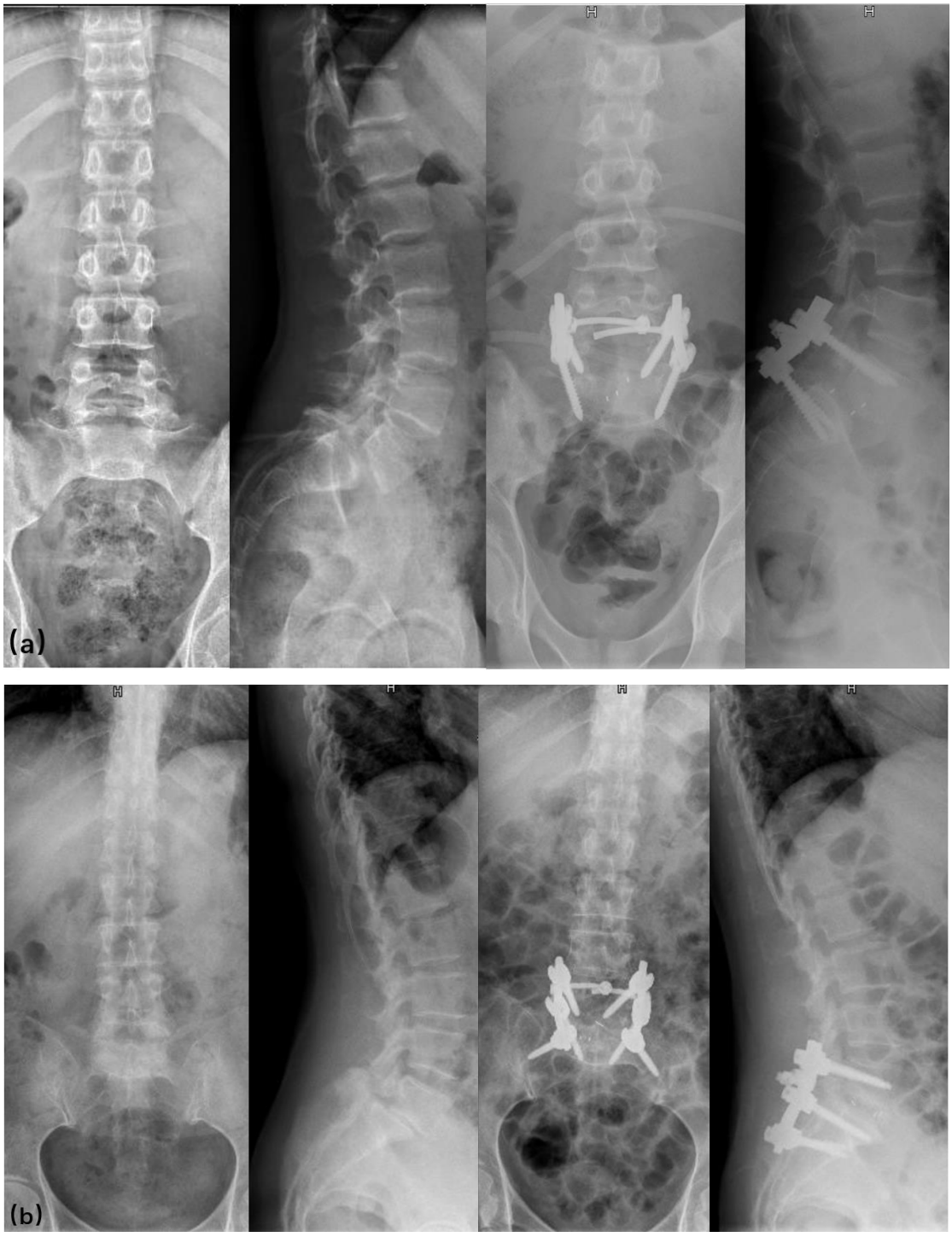

Fig.8 :(a) Preoperative and postoperative X-rays of spondylolisthesis patient treated with L5-S1 fixation; (b) Preoperative and postoperative X-rays of spondylolisthesis patient treated with L5-S2 alar fixation.

Regarding the stress of internal fixation, analysis of the S1 internal fixation stress in both models revealed that the S1 screw stress was concentrated at the tail of the screw in both groups and distributed on the upper and lower surfaces, while the S2 alar model showed relatively dispersed S1 screw stress. The upper surface of the screw showed bending stress, and the lower surface showed tensile stress. This indicates that during reduction, compression of the screw against the bone mainly occurs on the upper surface of the caudal segment of the screw path. Screw cutting and pull-out in the superoposterior direction could occur when the bone yield stress is reached. When subjected to the same reduction load, the stress of the S1 screw tail in the L5-S1 model was much higher than that in the L5-S2 alar model, predicting a higher risk of screw bending or even fracture. In the L5-S2 alar fixation model, the stress was highest on the connecting rod near the S1 screw, reaching 319-942 MPa at yield in different BMDs. However, it was still lower than the highest stress (423-945 MPa) of the S1 screw in the L5-S1 model at the same density. Therefore, the following can be concluded: 1. at the same BMD, the L5-S2 alar model had a higher risk of titanium rod deformation or even fracture, while the L5-S1 model had a higher risk of screw fracture; and 2. when the bone yield stress was reached, the risk of titanium rod deformation in the L5-S2 alar model was still lower than the risk of screw fracture in the L5-S1 model, which further proved that the overall structure of the L5-S2 alar model was more stable.

Regarding S1 screw path deformation, as the reduction load increased, there were different degrees of bone deformation in both models, mainly concentrated in

the anterior and caudal segments of the screw path, with downward compression deformation in the anterior segment and upward compression deformation in the caudal segment. The deformation of the screw path meant that compression fracture occurred in the bone, and the range of fracture increased with increasing reduction load. When the bone yield stress was reached, the average screw path deformation in the L5-S2 alar model was 60% to 100% higher than that in the L5-S1 model, while there was no significant difference in the maximum screw path deformation between the two models. The above results indicate the following: 1. with the same reduction effect (i.e., the same reduction load was applied) and the same BMD, in the L5-S2 alar model, the deformation of the S1 screw path was dispersed and uniform, while in the L5-S1 model, local bone destruction at the front and tail ends of the screw path easily occurred due to stress concentration; 2. when the bone yielded, the degree of screw path deformation had little correlation with bone density, according to Table 4; and 3. S1 screw loosening could occur with relatively minor bone destruction in the L5-S1 model, whereas it occurred with further bone compression in the L5-S2 alar model, indirectly proving that the L5-S2 alar model was more stable.

Unlike in the large majority of available finite element studies, we decided not to analyze only a group of single representative models but to construct a total of 72 models by fine-tuning the angle and depth of the screw to stimulate intraoperative errors. Although previous studies have reported the biomechanics of sacropelvic fixation [23,24], we first further discussed the advantages of the L5-S2 alar fixation

model in detail in severe spondylolisthesis patients with osteoporosis by setting different BMDs.

This study has some limitations. This model is only representative of a partial population and cannot fully reflect the lumbosacral conditions at different ages. Furthermore, to simplify the computations, only three overall BMD levels were set instead of reconstructing the lumbosacral bone according to the CT gray values. Moreover, the model did not consider the influence of the various muscle tissues and ligaments and thus cannot reflect the true in vivo conditions.

Conclusion

L5-S2 alar fixation can withstand a greater reduction load and has a relatively lower risk of rod or screw fracture. In summary, compared with L5-S1 fixation, extended fixation to the S2 alar has better stability and potential for improved reduction outcomes, especially in severe lumbar spondylolisthesis patients with severe osteoporosis.

Abbreviations

CT: Computed tomography; FEA: Finite element analysis; BMD: Bone mineral density; TLIF: Transforaminal lumbar interbody fusion; ANOVA: Analysis of variance.

Authors' contributions

All contributing authors have read and approved the manuscript in its present form. JHW – data collection, study design, data analysis and manuscript writing. WC – data collection, study design, data analysis and manuscript writing. XY – performing surgeries, study design. CZ – data collection, data analysis. TXL–data analysis. GJF –performing surgeries, supervising rehabilitation. YMS – performing surgeries, study supervisor, performing surgeries, study design and manuscript review. LML – study supervisor, performing surgeries, study design and manuscript review.

Acknowledgements

Not applicable.

Funding

This study was supported in part by the Projects of the Science & Technology Department of Sichuan Province: NO.2017SZ0046 and NO.2017SZDZX0021.

Availability of data and materials

The datasets used and/or analyzed during the current study are available from the corresponding author on reasonable request.

Ethics approval and consent to participate

This study was approved by the Ethics Committee of the West China Hospital. The participant consent was written and was performed in accordance with the ethical standards of the Declaration of Helsinki.

Consent for publication

Not applicable.

Competing interests

All authors declare that they have no competing interests

Reference

[1] Wiltse LL, Newman PH, Macnab I. Classification of spondylolisis and spondylolisthesis. Clin Orthop Relat Res. 1976;(117):23-29.

[2] Matthiass HH, Heine J. The surgical reduction of spondylolisthesis. Clin Orthop Relat Res. 1986;(203):34-44.

[3] Esses SI, Sachs BL, Dreyzin V. Complications associated with the technique of pedicle screw fixation. A selected survey of ABS members. Spine (Phila Pa 1976). 1993;18(15):2231-2239. doi:10.1097/00007632-199311000-00015

[4] Reinhold M, Schwieger K, Goldhahn J, Linke B, Knop C, Blauth M. Influence of screw positioning in a new anterior spine fixator on implant loosening in osteoporotic

vertebrae. Spine (Phila Pa 1976). 2006;31(4):406-413.
doi:10.1097/01.brs.0000199894.63450.70

[5] Krishnan V, Varghese V, Kumar GS. Comparative Analysis of Effect of Density, Insertion Angle and Reinsertion on Pull-Out Strength of Single and Two Pedicle Screw Constructs Using Synthetic Bone Model. Asian Spine J. 2016;10(3):414-421. doi:10.4184/asj.2016.10.3.414

[6] Birknes JK, White AP, Albert TJ, Shaffrey CI, Harrop JS. Adult degenerative scoliosis: a review. Neurosurgery. 2008;63(3 Suppl):94-103. doi:10.1227/01.NEU.0000325485.49323.B2

[7] Emami A, Deviren V, Berven S, Smith JA, Hu SS, Bradford DS. Outcome and complications of long fusions to the sacrum in adult spine deformity: luque-galveston, combined iliac and sacral screws, and sacral fixation. Spine (Phila Pa 1976). 2002;27(7):776-786. doi:10.1097/00007632-200204010-00017

[8] Orita S, Ohtori S, Eguchi Y, et al. Radiographic evaluation of monocortical versus tricortical purchase approaches in lumbosacral fixation with sacral pedicle screws: a prospective study of ninety consecutive patients. Spine (Phila Pa 1976). 2010;35(22):E1230-E1237. doi:10.1097/BRS.0b013e3181e5092c

[9] Morgan EF, Bouxsein ML. Use of finite element analysis to assess bone strength[J]. IBMS BoneKEy, 2005, 2:8.

[10] Lu T, Lu Y. Comparison of biomechanical performance among posterolateral fusion and transforaminal, extreme, and oblique lumbar interbody fusion: a finite element analysis. World Neurosurg. 2019;129:e890-e899.

[11] Chung SK, Kim YE, Wang KC. Biomechanical effect of constraint in lumbar total disc replacement: a study with finite element analysis[J]. Spine, 2009, 34(12):1281-1286.

[12] Brekelmans WA, Poort HW, Slooff TJ. A new method to analyse the mechanical behaviour of skeletal parts. Acta Orthop Scand. 1972;43(5):301-317. doi:10.3109/17453677208998949

[13] Belytschko T, Kulak RF, Schultz AB, Galante JO. Finite element stress analysis of an intervertebral disc. J Biomech. 1974;7(3):277-285. doi:10.1016/0021-9290(74)90019-0

[14] Liu YK, Ray G, Hirsch C. The resistance of the lumbar spine to direct shear. Orthop Clin North Am. 1975;6(1):33-49.

[15] Hakim NS, King AI. A computer-aided technique for the generation of a 3-D finite element model of a vertebra. Comput Biol Med. 1978;8(3):187-196. doi:10.1016/0010-4825(78)90019-7

[16] Chatzistergos PE, Magnissalis EA, Kourkoulis SK. A parametric study of cylindrical pedicle screw design implications on the pullout performance using an

417 experimentally validated finite-element model. Med Eng Phys. 2010;32(2):145-154.
418 doi:10.1016/j.medengphy.2009.11.003.

419 [17] Kashlan ON, Chen KS, La Marca F. Lumbosacral and Pelvic Fixation
420 Techniques[M]. In: Essentials of Spinal Stabilization. Holly LT, Anderson PA
421 (editors). Cham: Springer International Publishing; 2017. pp. 401-412.

422 [18] Koller H, Zenner J, Hempfing A, Ferraris L, Meier O. Reinforcement of
423 lumbosacral instrumentation using S1-pedicle screws combined with S2-alar screws.
424 Oper Orthop Traumatol. 2013;25(3):294-314. doi:10.1007/s00064-012-0160-0

425 [19] Lee SH, Jin W, Kim KT, Suk KS, Lee JH, Seo GW. Trajectory of transsacral
426 iliac screw for lumbopelvic fixation: a 3-dimensional computed tomography study. J
427 Spinal Disord Tech. 2011;24(3):151-156. doi:10.1097/BSD.0b013e3181e7c120

428 [20] Chang TL, Sponseller PD, Kebaish KM, Fishman EK. Low profile pelvic
429 fixation: anatomic parameters for sacral alar-iliac fixation versus traditional iliac
430 fixation. Spine (Phila Pa 1976). 2009;34(5):436-440.
431 doi:10.1097/BRS.0b013e318194128c

432 [21] Emami A, Deviren V, Berven S, Smith JA, Hu SS, Bradford DS. Outcome and
433 complications of long fusions to the sacrum in adult spine deformity: luque-galveston,
434 combined iliac and sacral screws, and sacral fixation. Spine (Phila Pa 1976).
435 2002;27(7):776-786. doi:10.1097/00007632-200204010-00017

[22] Kim JH, Horton W, Hamasaki T, Freedman B, Whitesides TE Jr, Hutton WC. Spinal instrumentation for sacral-pelvic fixation: a biomechanical comparison between constructs ending with either S2 bicortical, bitriangulated screws or iliac screws. J Spinal Disord Tech. 2010;23(8):506-512. doi:10.1097/BSD.0b013e3181c37438

[23] Galbusera F, Casaroli G, Chande R, et al. Biomechanics of sacropelvic fixation: a comprehensive finite element comparison of three techniques. Eur Spine J. 2020;29(2):295-305. doi:10.1007/s00586-019-06225-5

[24] Casaroli G, Galbusera F, Chande R, et al. Evaluation of iliac screw, S2 alar-iliac screw and laterally placed triangular titanium implants for sacropelvic fixation in combination with posterior lumbar instrumentation: a finite element study. Eur Spine J. 2019;28(7):1724-1732. doi:10.1007/s00586-019-06006-0